Stem Cell Reports

Supplemental Information

Activated STAT5 Confers Resistance to Intestinal Injury by Increasing Intestinal Stem Cell Proliferation and Regeneration

Shila Gilbert, Harini Nivarthi, Christopher N. Mayhew, Yuan-Hung Lo, Taeko K. Noah, Jefferson Vallance, Thomas Rülicke, Mathias Müller, Anil G. Jegga, Wenjuan Tang, Dongsheng Zhang, Michael Helmrath, Noah Shroyer, Richard Moriggl, and Xiaonan Han

Figure S1

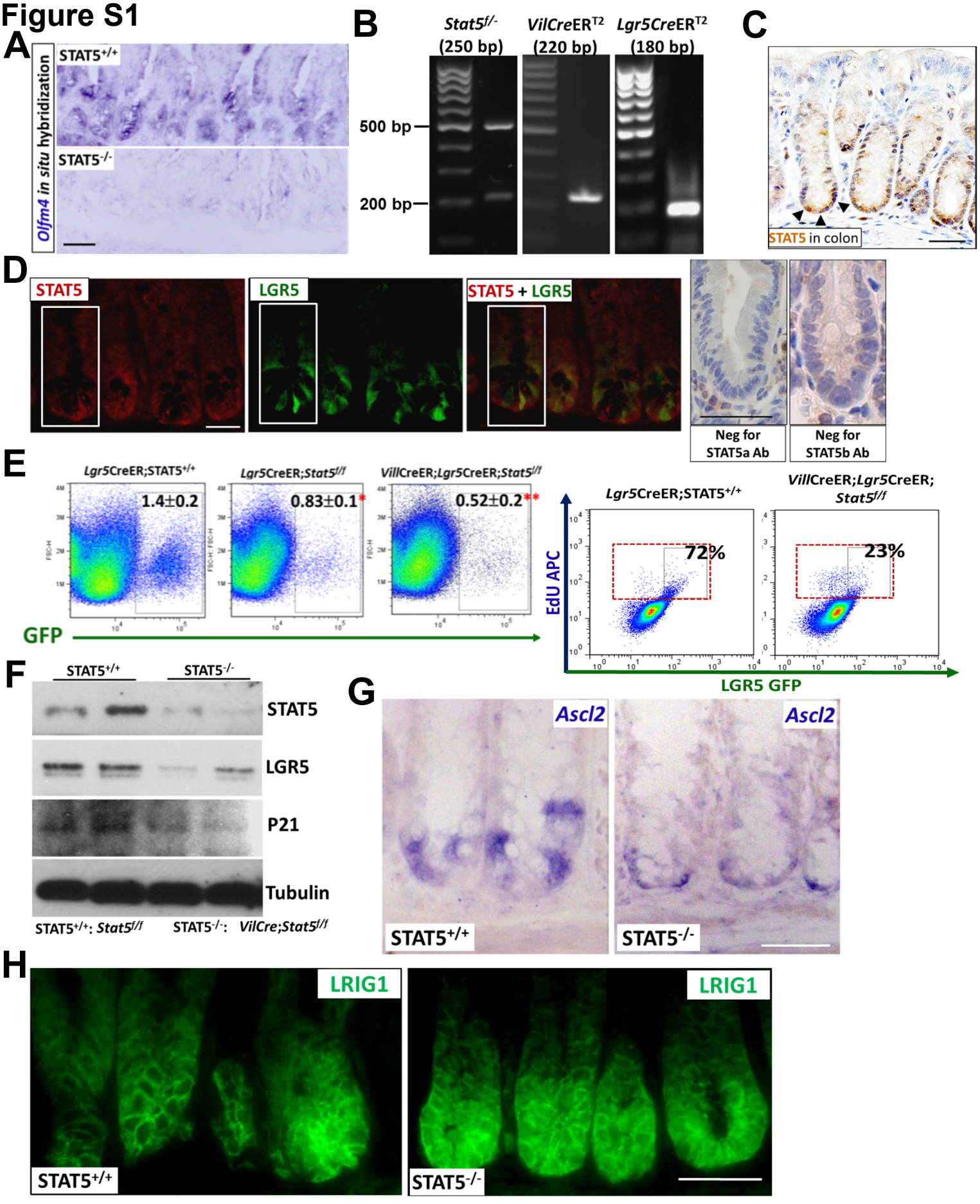
A
Olfm4 in situ hybridization
STAT5+/+
STAT5-/-
B
Stat5f/- (250 bp)
VilCreER T2 (220 bp)
Lgr5CreER T2 (180 bp)
500 bp
200 bp
C
STAT5 in colon
D
STAT5
LGR5
STAT5 + LGR5
Neg for STAT5a Ab
Neg for STAT5b Ab
E
Lgr5CreER;STAT5+/+
Lgr5CreER;Stat5f/f
VillCreER;Lgr5CreER;Stat5f/f
1.4±0.2
0.83±0.1*
0.52±0.2**
GFP
EdU APC
72%
23%
LGR5 GFP
F
STAT5+/+
STAT5-/-
STAT5
LGR5
P21
Tubulin
STAT5+/+: Stat5f/f
STAT5-/-: VilCre;Stat5f/f
G
Ascl2
STAT5+/+
STAT5-/-
H
LRIG1
STAT5+/+
STAT5-/-

Figure S1. Related to Figure 1.

A) *In situ* hybridization analysis for *Olfm4* in the crypts from STAT5$^{-/-}$ mice is shown, n≥4 mice per group.

B) Inducible depletion of STAT5 from LGR5^{+} IESCs was achieved by breeding *Stat5*$^{f/f}$ mice with *Lgr5Cre*ER transgenic mice and *VilCre*ER^{T2} transgenic mice. PCR genotyping was used to genotype the existence of *Stat5*$^{f/f}$, *Lgr5Cre*ER^{T2} and *VilCre*ER^{T2} in mice.

C) Colonic STAT5 expression was determined by immunohistochemistry staining (IH), the arrows indicate STAT5 expression at the crypt base. Original magnification × 400, n=3 mice.

D) Ileal frozen sections from *Lgr5* reporter mice were co-stained with STAT5 (red) and LGR5-GFP (green) in multiple crypts (left panel). Negative controls (Neg) show the staining specificity of STAT5a or STAT5b antibodies by staining STAT5 deficient intestine (right panel). Data represent three independent experiments.

E) IECs were dissociated. Frequency of LGR5 GFP^{+} (left panel) and LGR5 GFP^{+}EdU^{+} IECs in the EdU^{+} IECs (right panel) were measured by FACS. Representative scatter graphs are shown. Results are expressed as the mean ± SEM, n=4 or 6 mice per group, * $p < 0.05$ and ** $p < 0.01$ vs *Lgr5Cre*ER;STAT5$^{+/+}$ mice.

F) Constitutive IEC-STAT5 deficient (STAT5$^{-/-}$) mice were generated using Cre-mediated recombination to delete *Stat5* locus in colonic IECs. Colonic IECs were isolated from STAT5$^{+/+}$ and STAT5$^{-/-}$ mice, STAT5, LGR5, and P21 expression were identified with immunoblotting, n=5 mice per group.

G) *Ascl2* expression in colonic IECs in STAT5$^{+/+}$ and STAT5$^{-/-}$ mice was determined by *In Situ* Hybridization, n=4 mice per group.

H) LRIG1 in the colonic IECs was identified with immunofluorescence staining, n=5 mice per group.

Scale bars, 50 μm.

Figure S2

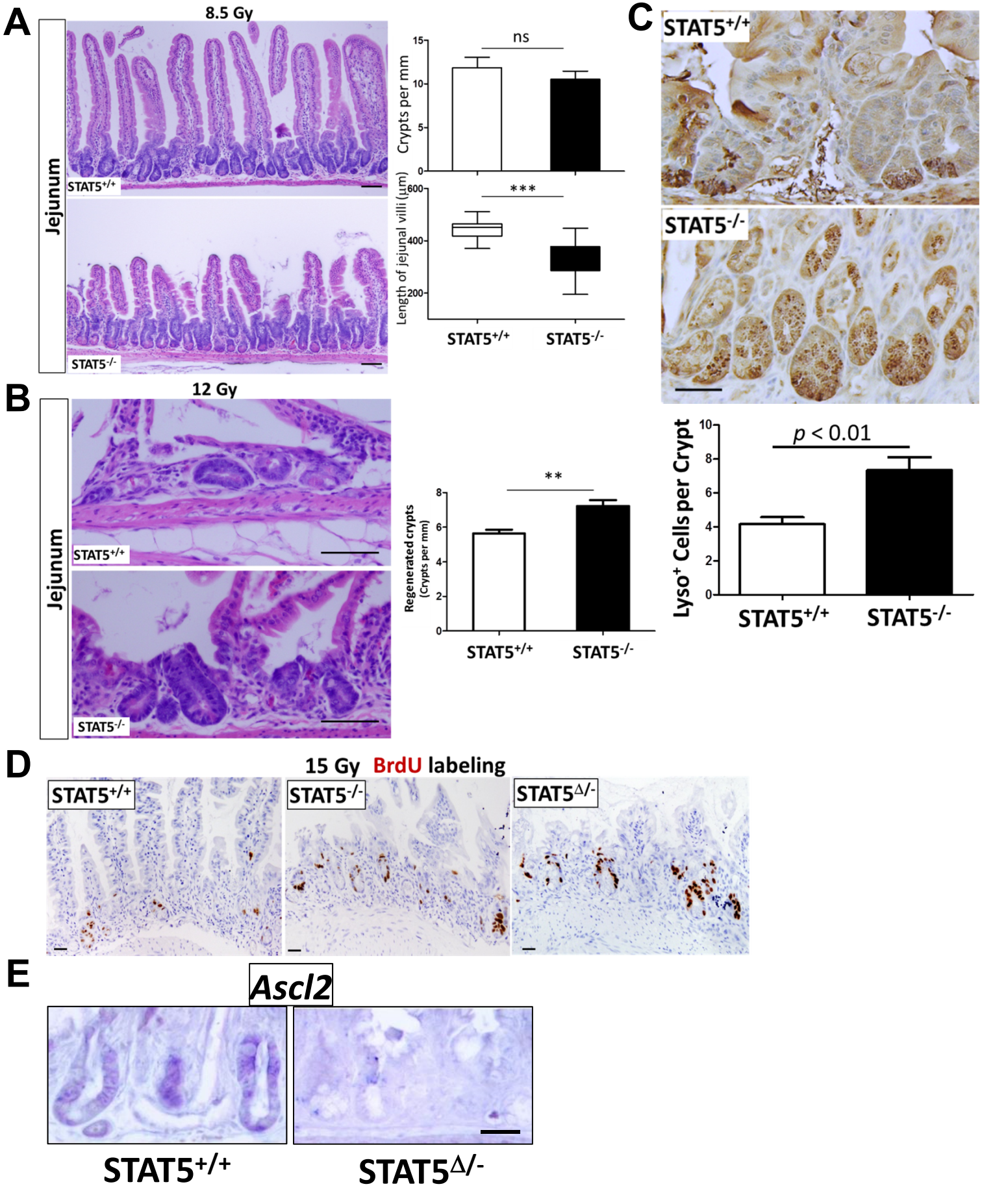
A
8.5 Gy
Jejunum
STAT5+/+
STAT5-/-
Crypts per mm
ns
Length of jejunal villi (µm)
***
STAT5+/+
STAT5-/-
B
12 Gy
Jejunum
STAT5+/+
STAT5-/-
Regenerated crypts (Crypts per mm)
**
STAT5+/+
STAT5-/-
C
STAT5+/+
STAT5-/-
Lyso+ Cells per Crypt
p < 0.01
STAT5+/+
STAT5-/-
D
15 Gy BrdU labeling
STAT5+/+
STAT5-/-
STAT5Δ/-
E
Ascl2
STAT5+/+
STAT5Δ/-

Figure S2. Related to Figure 2.

A,B) $STAT5^{-/-}$ or $STAT5^{+/+}$ mice were exposed to γ-radiation (8.5 or 12 Gy). Jejunal crypt proliferation and length of villi were determined after 3.5 day-recovery following an initial 8.5-Gy irradiation (A) or crypt regeneration was determined after 3.5 day-recovery following 12-Gy irradiation (B). Results are expressed as the mean ± SEM, n=6 mice per group, ** $p < 0.01$. Whiskers represent minimum and maximum values.

C) Paneth cells were immunostained with Lysozyme. $Lysozyme^{+}$ Paneth cells were counted in both properly oriented and distorted crypts. The results were expressed as $Lysozyme^{+}$ cells per crypt, n=5 mice per group. Original magnification × 200.

D) $STAT5^{-/-}$ or $STAT5^{\Delta/-}$ mice were respectively exposed to 15 Gy radiation. 3.5 days post-radiation, these mice were administered with BrdU and sacrificed 3 hours later. Representative images of BrdU incorporation are shown, n=5 mice per group.

E) *In situ* hybridization analysis for *Ascl2* in the crypts from irradiated $STAT5^{+/+}$ and $STAT5^{\Delta/-}$ mice is shown, n=4 mice per group.

Scale bars, 50 μm.

Figure S3

A

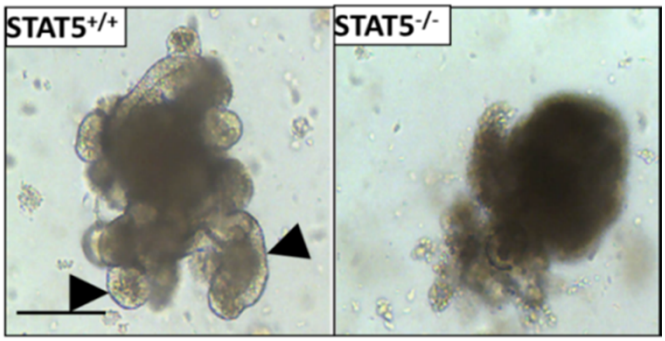

7 days

B

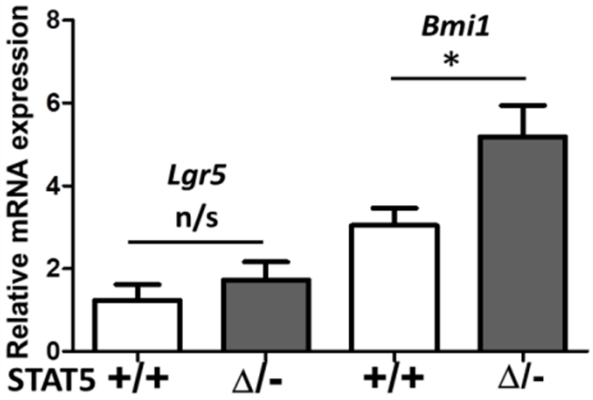

Figure S3. Related to Figure 3.

A) Ileal crypts were isolated from STAT5$^{-/-}$ or STAT5$^{+/+}$ mice, and resuspended in matrigel with EGF, Noggin and R-spondin to culture them for 7 days. Representative images are shown. Data are representatives of three independent experiments. Scale bars, 100 μm.

B) RNA was extracted from 7 day-old enteroids, *Lgr5* and *Bmi1* mRNA levels were determined by qPCR. Results are expressed as the mean ± SEM, n=5 mice per group, * $p<0.05$.

Figure S4

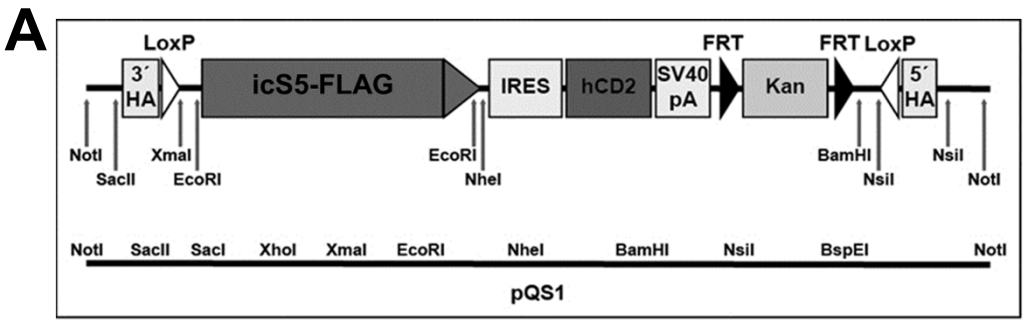
A
LoxP
3´ HA
icS5-FLAG
IRES
hCD2
SV40 pA
FRT
Kan
FRT
LoxP
5´ HA
NotI
SacII
XmaI
EcoRI
EcoRI
NheI
BamHI
NsiI
NsiI
NotI
NotI SacII SacI XhoI XmaI EcoRI NheI BamHI NsiI BspEI NotI
pQS1

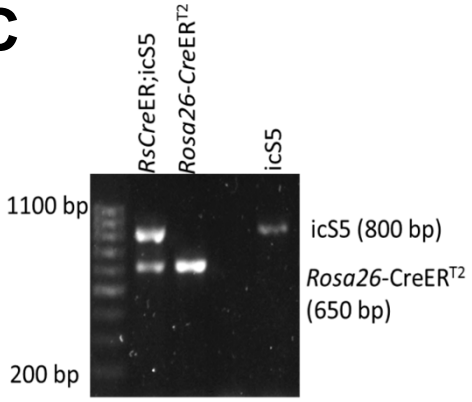
C
RsCreER;icS5
Rosa26-CreER^{T2}
icS5
1100 bp
200 bp
icS5 (800 bp)
Rosa26-CreER^{T2} (650 bp)

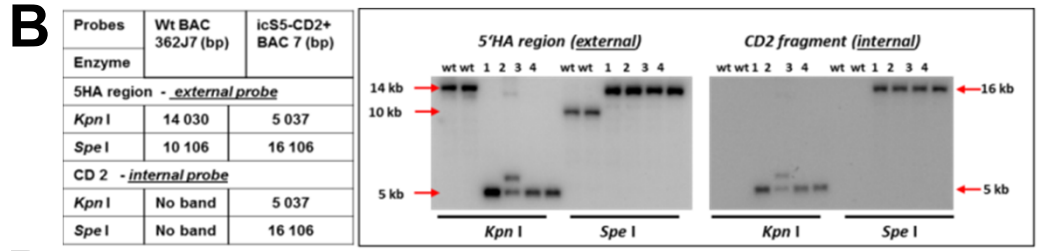
B
Probes
Enzyme
Wt BAC 362J7 (bp)
icS5-CD2+ BAC 7 (bp)
5HA region - external probe
Kpn I 14 030 5 037
Spe I 10 106 16 106
CD 2 - internal probe
Kpn I No band 5 037
Spe I No band 16 106
5'HA region (external)
CD2 fragment (internal)
wt wt 1 2 3 4 wt wt 1 2 3 4
wt wt 1 2 3 4 wt wt 1 2 3 4
14 kb
10 kb
5 kb
16 kb
5 kb
Kpn I
Spe I
Kpn I
Spe I

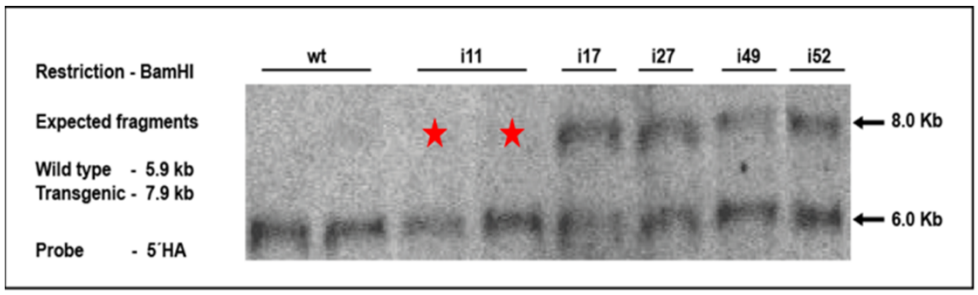
D
Restriction - BamHI
Expected fragments
Wild type - 5.9 kb
Transgenic - 7.9 kb
Probe - 5´HA
wt
i11
i17
i27
i49
i52
8.0 Kb
6.0 Kb

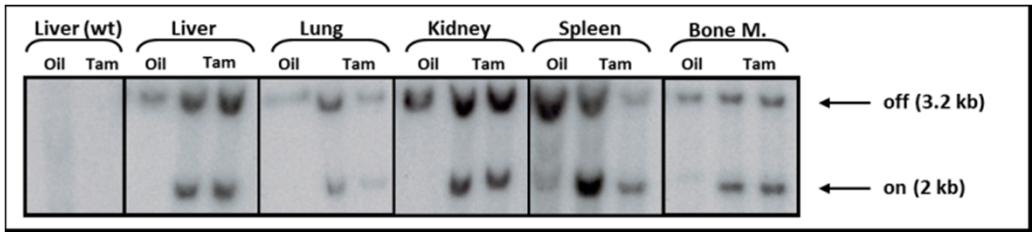
E
Liver (wt)
Liver
Lung
Kidney
Spleen
Bone M.
Oil Tam Oil Tam Oil Tam Oil Tam Oil Tam Oil Tam
off (3.2 kb)
on (2 kb)

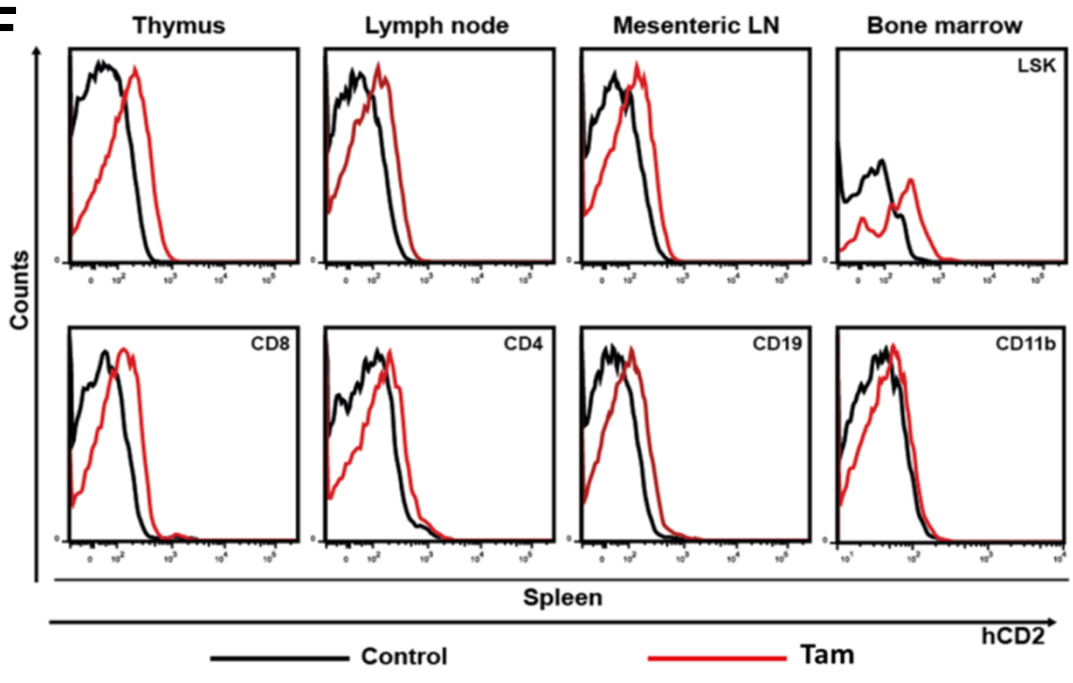
F
Thymus
Lymph node
Mesenteric LN
Bone marrow
LSK
CD8
CD4
CD19
CD11b
Counts
Spleen
hCD2
Control
Tam

Figure S4. Related to Figure 4.

A) Schematic diagram of icS5-IRES-hCD2 construct. This plasmid was used to introduce the icS5-IRES-hCD2 sequence into the wild type BAC, by homologous recombination using the 5'HA and 3'HA sequences, in an orientation opposite to the transcriptional direction.

B) 2 bacterial colonies with wild type BAC and 4 colonies with recombinant BAC were digested with two different enzymes (Kpnl and Spel). Southern blotting was used to confirm BAC recombination. The membranes were probed with radioactively labeled probes against the 5' homologues arm region and hCD2 region. Fragments of expected size were seen, confirming the recombined BAC constructs with the icS5-IRES-hCD2 sequence.

C) Generation of transgenic mice with inducible activation of STAT5. Genotypes of *Rosa26*-CreER^{T2} ,icS5 and *RsCre*ER;icS5 mice were determined by PCR.

D) Southern blot analysis of icS5 transgenic mice. Southern blot was performed with the tail DNA from icS5 transgenic mice. 5'HA sequence was used as probe. Fragments of expected size of the endogenous locus were seen in all mice but not i11 (see red star labels). These analyses suggest that only a piece of the BAC has integrated in this mouse. Intensity of the endogenous and transgenic bands suggests a low copy number (one up to two copies) in all four mice.

E) Genomic recombination of icS5 constructs. Upon treatment of *RsCre*ER;icS5 mice with Tam, recombination of the genomic locus was seen in different organs, as detected by Southern blotting. n=3 mice per group.

F) hCD2 expression upon induction of *RsCre*ER;icS5 mice. FACS analysis of the cells showed low levels, but consistent expression of hCD2 transgene in the different hematopoietic organs: spleen, thymus, lymph nodes, mesenteric lymph nodes and bone marrow. The black line represents hCD2 expression in control mice while the red line represents hCD2 in Tam-induced mice. In spleen, hCD2 was detected in T-cells ($CD4^+$ and $CD8^+$) and B cells ($CD19^+$). However, no expression was seen in myeloid cells ($CD11b^+$). In the bone marrow, hCD2 expression can be seen in the early progenitor (LSK) cells after Tam induction, n=3 mice per group.

Figure S5

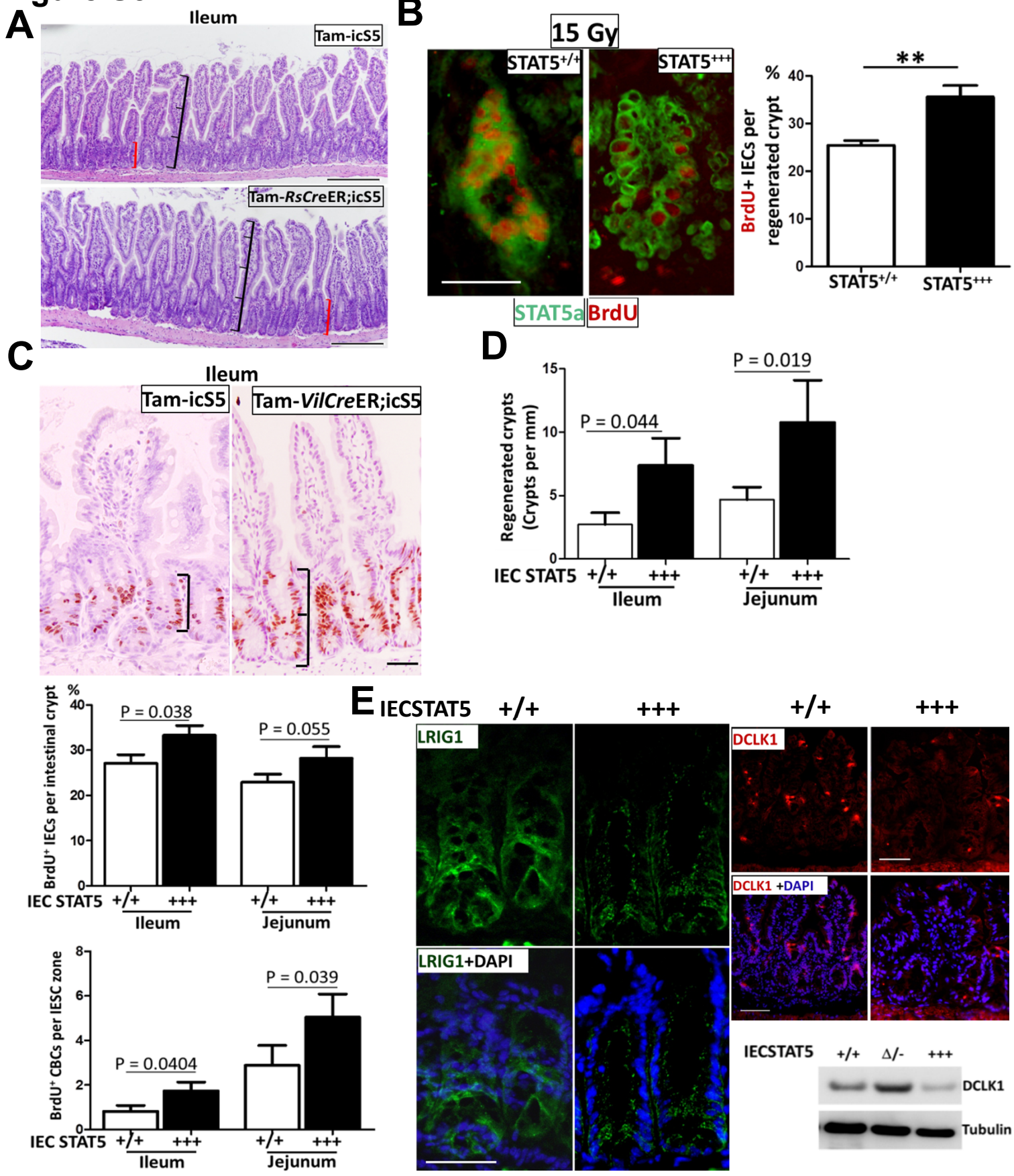
A
Ileum
Tam-icS5
Tam-RsCreER;icS5
B
15 Gy
STAT5+/+
STAT5+++
STAT5a
BrdU
BrdU+ IECs per regenerated crypt
**
STAT5+/+
STAT5+++
C
Ileum
Tam-icS5
Tam-VilCreER;icS5
D
Regenerated crypts (Crypts per mm)
P = 0.044
P = 0.019
IEC STAT5
Ileum
Jejunum
BrdU+ IECs per intestinal crypt
P = 0.038
P = 0.055
BrdU+ CBCs per IESC zone
P = 0.0404
P = 0.039
E
IECSTAT5
LRIG1
LRIG1+DAPI
DCLK1
DCLK1 +DAPI
Δ/-
Tubulin

Figure S5. Related to Figure 4.

A) Hematoxylin and Eosin staining (HE) with ileal tissues shows that the villi in Tam-*Rs*CreER;icS5 mice are significantly elongated compared to Tam-icS5 mice. Original magnification × 100, scales represent ileal villus (black) or crypt (red) length.

B) $STAT5^{+/+}$ and $STAT5^{+++}$ mice were exposed to the γ-radiation. 3.5 days after an initial 15-Gy radiation, ileal regenerated crypts were double-stained with STAT5a (green) and BrdU (red) IF. The representative images were shown, n=6 mice per group. Percentages of proliferative IECs in the regenerated crypt were measured by BrdU incorporation. Results are expressed as the mean ± SEM (n=5 mice per group), ** $p < 0.01$.

C) icS5 mice were crossed with *VilCre*ER^{T2} (*VilCre*ER;icS5). STAT5 was activated by 5-day Tam induction. IEC or CBC proliferation was quantified by *in situ* BrdU labeling, and is respectively expressed as $BrdU^+$ IECs per crypt or $BrdU^+$ IESC per stem cell zone. Results are expressed as the mean ± SEM (n=4 or 5 mice per group).

D) *VilCre*ER;icS5 and icS5 mice were exposed to the γ-radiation. 3.5 day after an initial 15 Gy radiation, crypt regeneration was determined. Results are expressed as the mean ± SEM (n=5 mice per group).

E) Ileal frozen sections from $STAT5^{+/+}$ and *VilCre*ER;icS5 mice were immunostained with anti-LRIG1 (green), DCLK1 (red), and DAPI (Blue), n≥5 mice per group. Ileal IECs were isolated from $STAT5^{+/+}$, *VilCre*ER;$Stat5^{f/f}$ and *VilCre*ER;icS5 mice. DCLK1 protein expression was identified with immunoblotting (n=3 mice per group).

Scale bars, 50 μm.

Figure S6

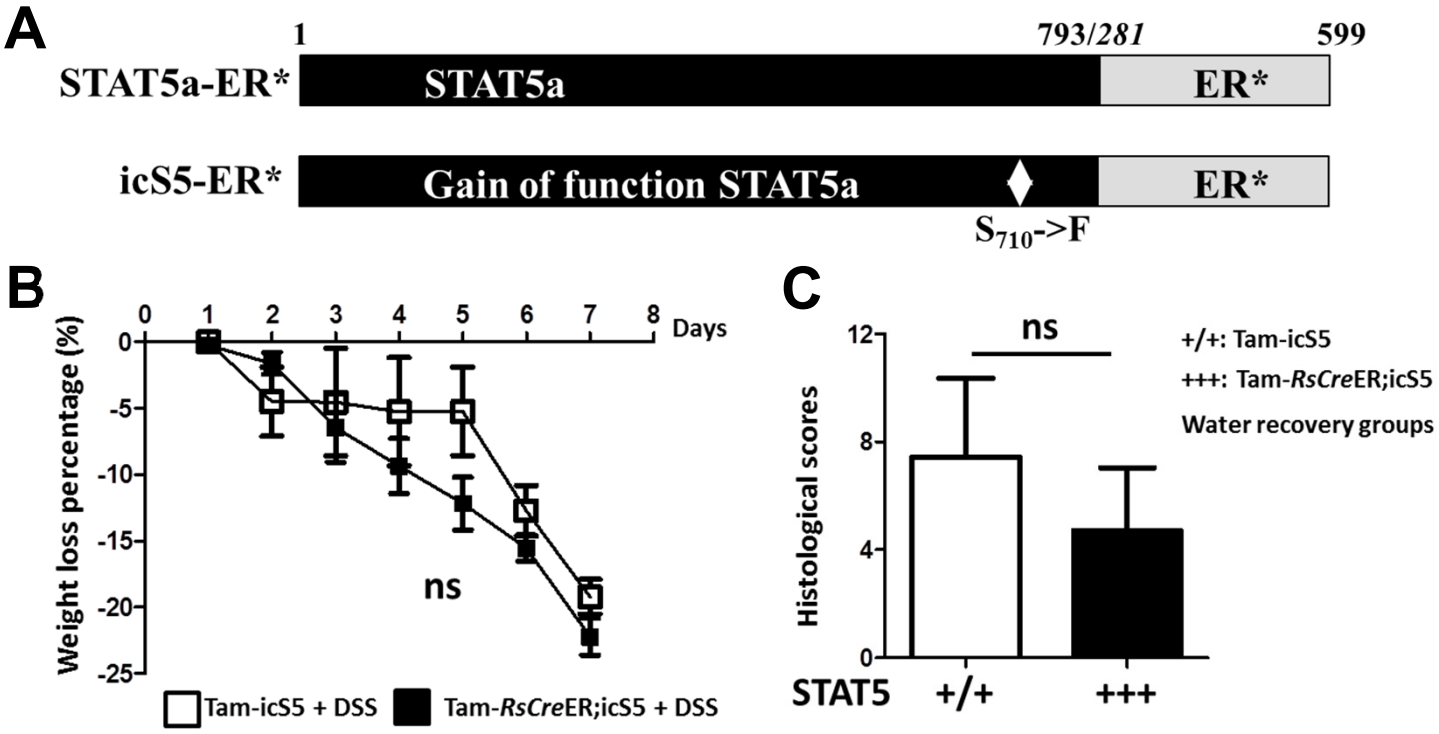
A
1
793/281
599
STAT5a-ER*
STAT5a
ER*
icS5-ER*
Gain of function STAT5a
ER*
S710->F
B
Weight loss percentage (%)
0
-5
-10
-15
-20
-25
0 1 2 3 4 5 6 7 8
Days
ns
Tam-icS5 + DSS
Tam-RsCreER;icS5 + DSS
C
Histological scores
12
8
4
0
ns
STAT5
+/+
+++
+/+: Tam-icS5
+++: Tam-RsCreER;icS5
Water recovery groups

Figure S6. Related to Figure 5 and Figure 7.

A) Structures of wild type STAT5a and constitutively active mutant of STAT5a (icS5) constructs. The GOF STAT5a in Ser710/Phe (icS5) mutation causes enhanced and prolonged tyrosine phosphorylation in a Tam dose dependent fashion.

B) Acute colonic inflammation was induced by 3% DSS for 7 days in Tam-induced icS5 or *RsCre*ER;icS5 mice. Percentage of weight loss was measured daily. Results are expressed as the mean ± SEM, n=6 mice per group, ns=non-significant

C) Tam-induced icS5 or *RsCre*ER;icS5 mice were orally administered with 3% DSS for 5 days followed by 5 day water recovery. Colonic inflammation was scored, results are expressed as the mean ± SEM, n=6 or 8 mice per group.

Supplemental Tables

Table S1

A

Putative STAT5 binding sites in the human *BMI1* locus (consensus: TTCNNNGAA)	Position relative to TSS
TTCTAGGAA	+3089
TTCAAGGAA	+3519
TTCTGTGAA	+5193
TTCACAGAA	+5864
TTCTCAGAA	+7460
TTCTTGGAA	+8553

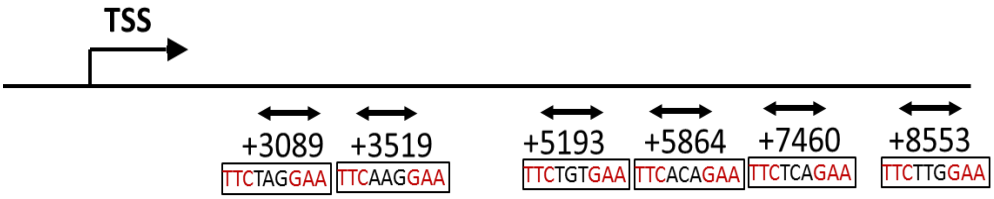

B

Primers	Sequences
*BMI1*_1	5'-TGGAGCCCCTTCATGAACTT-3' 5'-GCACGGAGGAGTTGTAGGTA-3'
*BMI1*_2	5'-CAGCCATTGAGCTGTGTTGA-3' 5'-CCGACAGTCAGGGAAGTCAA-3'
*BMI1*_3	5'-GCCCAGCTGTACAGTGTTAA-3' 5'-TCAGGTGGGGATTTAGCTCA-3'
*BMI1*_4	5'-TGTTCGTTACCTGGAGACCA-3' 5'-TAAACGGCTACCCTCCACAA-3'
*BMI1*_5	5'-TGTTTGGATCTGAGTTCGTGTG-3' 5'-AGGAGATCGCATCGTTTCCT-3'

Table S1

A) Putative STAT5 binding sites in the human *BMI1* locus (consensus: TTCNNNGAA).

Positions relative to the TSS of *BMI1* are shown.

B) Primer sequences of putative STAT5 binding sites in the human *BMI1* locus.

Table S2

A

PutativeSTAT5 binding sites in the mouse *Bmi1* locus (consensus: TTCNNNGAA)	Position relative to TSS
TTCCAAGAA	-8952
TTCCATGAA	-5926
TTCGGAGAA	+1427
TTCTATGAA	+1949
TTCAGTGAA	+5899
TTCTGAGAA	+7675

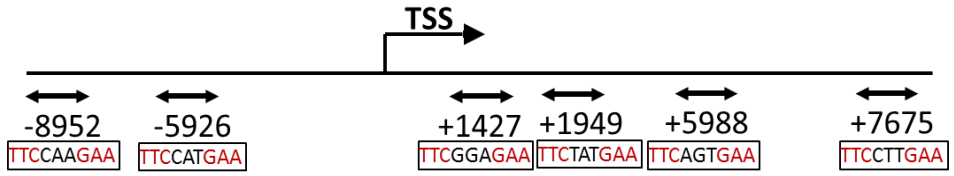

B

Primers	Sequences
Cis	5’-GTCCAAAGCACTAGACGCCTG-3’ 5’-TTCCCGGAAGCCTCATCTT-3’
*Bmi1*_1	5’-CGACCATCTCCTGACCATCA-3’ 5’-AAGAATGGGCTGGATCCTGG-3’
*Bmi1*_2	5’-AAGCAGAGAAGTAGGGGTGG-3’ 5’-GCACGTTGTCACATTGGACA-3’
*Bmi1*_3	5’-CCACTCTCACCCCTCCTTTT-3’ 5’-AAGCTCTGGGGAAACGATCA-3’
*Bmi1*_4	5’-TGGGTCCTAAGTACACTAGGGA-3’ 5’-TGATGGGGAGAACTTTGCCT-3’
*Bmi1*_5	5’-GCATGCCTACCCAAACCTTAG-3’ 5’-GACGGGTGAGCTGCATAAAA-3’

Table S2

A) PutativeSTAT5 binding sites in the mouse *Bmi1* locus (consensus: TTCNNNGAA).

B) Primer sequences of putative STAT5 binding sites in the mouse *Bmi1* locus. Positions relative to the TSS of *Bmi1* are shown.

Table S3

Primers for qPCR	Sequences
Lgr5	5'-CGGAGGAAGCGCTACAGAAT-3' 5'-CTGGGTGGCACGTAGCTGAT-3'
Bmi1	5'-GGGCTTTTCAAAAATGAGATGAA-3' 5'- GAGCCATTGGCAGCATCAG-3'
GAPDH	5'-GGTGGGTGGTCCAAGGTTTC-3' 5'-TGGTTTGACAATGAATACGGCTAC-3'

Table S3

Primer sequences for real time PCR of mRNA transcripts analyzed.

Supplemental Experimental Procedures

Materials. All chemicals were purchased from Sigma-Aldrich (St. Louis, MO) unless otherwise noted. Antibodies specific for BMI1 (Cat # 5856) and tyrosine phosphorylation specific STAT5 antibodies (PY-STAT5, Cat # 4322) used for immunohistochemistry staining were purchased from Cell Signaling Technology (Boston, MA), antibodies specific for LGR5 from OriGene (Cat # TA503316, Rockville, MD), antibodies specific for LRIG1 from R&D (Cat # AF3688, Minneapolis, MN), antibodies specific for Lysozyme (Cat # A0099) and Ki67 (Cat # M7249) from Dako (Carpinteria, CA), antibodies specific for GFP (Cat # ab13970) and DCLK1 (Cat # ab31704) from Abcam (Cambridge, MA), antibodies specific for STAT5a (Cat # 71-2400) and STAT5b (Cat # 71-2500) from Zymed Laboratories (Life Technologies, Grand Island, NY), and antibodies specific for total STAT5 (Cat # sc-835) and β-tubulin (Cat # sc-9104) from Santa Cruz Biotechnology (Santa Cruz, CA). Tyrosine phosphorylation specific STAT5 antibody (Tyr642/699) used for immunoblotting was from Upstate Biotechnology (Cat # 05-495, Lake Placid, NY). For stem cell culture, matrigel was purchased from BD Biosciences (San Jose, CA), and EGF, Noggin and R-spondin were from R&D, advanced DMEM/F12 media were from Life Technologies, and mTeSR1 media were from STEMCELL Technologies (Vancouver, Canada). For lentiviral transduction reagents, pLENTI-PGK-Puro-DEST (w529-2) plasmids were from Addgene (Cambridge, MA), iProof High-Fidelity DNA Polymerase was from Life Science Research (Hercules, CA) and pENTR/D-TOPO cloning kit from Life Technologies (Grand Island, NY). ChIP kit for human cells was from Upstate Biotechnology (Lake Placid, NY). Anti-FLAG antibodies for mouse ChIP assay were from Sigma and Dynabeads Protein G from Life Technologies. Normal mouse IgG was purchased from Millipore (Billerica, MA). BrdU *in situ* detection kit was purchased from BD Biosciences. TUNEL *in situ* apoptotic detection kit was

from Millipore. Click-iT EdU Alexa Fluor® 647 FACS and Imaging Kits were purchased from Life Technologies.

Animal resources and maintenance: The animal study protocol has been approved by the CHRF Institutional Animal Care and Use Committee (IACUC, 1E03030). Breeding pairs for transgenic mice with icS5 mice (icS5) and *Rosa26-Cre*ER^{T2} were obtained from Dr. Moriggl at LBI-CR, Vienna, Austria. Breeding pairs of *Stat5*$^{f/f}$ were from Dr. Hennighausen at NIDDK (Cui et al., 2004). *Villin-Cre*ER^{T2} mice were obtained from Dr. Zheng at CCHMC (Melendez et al., 2013). LGR5 reporter mice (*Lgr5*-EGFP-IRES-CreER^{T2}) mice were from Dr. Shroyer at CCHMC (Barker et al., 2007; Yan et al., 2012). C57BL/6 and *Villin-Cre* transgenic mice were ordered from Jackson Labs (Bar Harbor, MA). Constitutive or inducible depletion of STAT5 from intestinal epithelia was achieved by breeding *Stat5*$^{f/f}$ mice with *Villin*-Cre or *Villin*-CreER^{T2} transgenic mice (el Marjou et al., 2004); inducible hyper-activation of STAT5 was generated by breeding icS5 mice with *Rosa26-Cre*ER^{T2} or *Villin-Cre*ER^{T2} transgenic mice (Hameyer et al., 2007). The effects of inducible depletion of STAT5 upon LGR5^{+} IESCs were investigated through crossing *Stat5*$^{f/f}$ mice with *Lgr5*-eGFP-IRES-CreER^{T2} and *Villin-Cre*ER^{T2} mice, by which Tam induction can efficiently deplete STAT5 in LGR5^{+} IESCs (Kim et al., 2012) (Figure S1B). All mice used in these studies have been backcrossed with C57BL/6 for more than ten generations and were re-genotyped with respect to STAT5 and Cre prior to necropsy. All studies were performed with littermate *Stat5*$^{f/f}$ or icS5 mice designated as wild-type controls, *Stat5*$^{f/f}$ mice with *Villin*-Cre or *Villin-Cre*ER^{T2} denoted as *VilCre;Stat5*$^{f/f}$ or *VilCre*ER;*Stat5*$^{f/f}$ mice, and icS5 mice with *Rosa26-cre*ER^{T2} or *Villin-Cre*ER^{T2} mice denoted as *RsCre*ER;icS5 or *VilCre*ER;icS5 mice were maintained in specific pathogen free (SPF) conditions in the Children's Hospital Research Foundation (CHRF) and CCHMC Animal Care Facility.

Radiation-induced injury models. Eight-week old knockout or transgenic mice were exposed to 8.5, 12 or 15 Gy whole body γ-radiation for 10 minutes at Comprehensive Mouse and Cancer Core, CCHMC (Hua et al., 2012). 3.5 day post-radiation, the mice were intraperitoneally administered with BrdU or EdU and then euthanized three hours later. The intestinal tissues were inspected for gross and histological abnormalities (Han et al., 2010; Hua et al., 2012). Radiation Injury Scores (RIS) and mucosal ulceration of radiation-induced intestinal mucositis were determined as published (Akpolat et al., 2009). RIS is a composite histopathologic scoring system that was extensively improved by our laboratory. Briefly, Scores of γ-radiation-induced ileal mucosal damage (scores: 1, 2 and 3), crypt loss (scores: 1, 2 and 3), mucosal ulcerations (scores: 1, 2 and 3), and thickening of intestinal wall (scores: 1, 2 and 3) were combined as RIS. Numbers of proliferating crypts or regenerated crypts ("microcolonies") were quantified as crypts per mm under microscope (magnification 100 ×) and were confirmed by BrdU labeling.

Animal model of colitis. Intestinal inflammation was induced by providing transgenic or control littermate mice with 3% dextran sulphate sodium (DSS) water (m.w. 36,000–50,000; MP Biomedicals) for either 7 days for acute injury studies or 5 days followed by 5 days of water for healing studies. Mice were sacrificed three hours after BrdU administration; the colon was removed. Scoring parameters included quantitation of the area of middle and distal colon involved, edema, erosion/ulceration of the epithelial monolayer, crypt loss/damage and infiltration of immune cells into the mucosa. Total disease score was expressed as the mean of all combined scores per genotype (Gilbert et al., 2012).

Enteroid culture and differentiation. Mouse crypt-derived enteroids are used as a model to study IESC proliferation and differentiation (Sato et al., 2009). Jejunal and ileal crypts were isolated from *Stat5*$^{f/f}$, *VilCre*ER;*Stat5*$^{f/f}$, *VilCre*ER;*Lgr5Cre*ER;*Stat5*$^{f/f}$, *RsCre*ER;icS5, and

*RsCre*ER;*Lgr5Cre*ER;icS5 mice, and then dissociated with Chelation Buffer (1 mM EDTA, 5 mM EGTA, 0.5 mM DTT, 43.3 mM Sucrose, and 54.9 mM Sorbitol). The crypts are filtered and re-suspended in Matrigel with 50 ng/ml EGF, 100 ng/ml Noggin, and 500ng/mL R-spondin. IESCs were *in vitro* differentiated from day 1 to day 14 as published (Sato et al., 2009; Spence et al., 2011). Different doses of 4-hydroxy-tamoxifen (200 nM or 1 μM, 4HT) were used to induce STAT5 activation or depletion in the mouse enteroids. Stem cell dividing process was imaged and recorded with an inverted microscope (Olympus TH4-100, Japan). Enteroids were cultured in six parallel wells per mouse for each experiment ($n \geq 4$ mice per group). The number of crypt buds from a minimum of 10 enteroids per well was determined and expressed graphically as the number of crypt buds *vs*. time.

Immunoblotting, Immunofluorescence, Immunohistochemistry, *In Situ* Hybridization (*In Situ*), and TUNEL assay. Isolated colonic and ileal IECs, and mucosal tissue were saved. Total cellular protein (TP), cytosolic protein (CE) and nuclear protein (NE) extracts were prepared using cold RIPA buffer and the NE-PER kit per the manufacturers' recommendations (Pierce, Rockford, IL). Expression of LGR5, BMI1, LRIG1, DCLK1, and CYCLIN D1 were measured in TP. The nuclear abundance of PY-STAT5 (Upstate Biotechnology) and STAT5a were detected in NE (Gilbert et al., 2012). Frozen tissue sections from mouse ileum and colon (4 μm) were prefixed in paraformaldehyde. Tissue sections were labeled with LRIG1 (Wong et al., 2012), DCLK1, BMI1 (Munoz et al., 2012), and Lysozyme antibodies following FITC-conjugated or TRITC-conjugated anti-rabbit secondary antibodies, 4,6-diamidino-2-phenylindole dihydrochloride (DAPI) were used for nuclear counterstaining. STAT5a, STAT5b, PY-STAT5 (Cell Signaling) and Ki67 (Daka) were examined in paraffin embedded intestinal sections using VECTASTAIN Elite ABC system (Vector lab, Burlingame, CA). The mRNA levels of *Olfm4*

(plasmid clone: 4163833) and *Ascl2* (plasmid clone: 1078130) in intestinal crypts were determined with *In Situ* hybridization (Gregorieff and Clevers, 2010). BrdU staining followed manufacturer's instructions (BrdU *in situ* Detection Kit, BD Pharmingen) (Gilbert et al., 2012). EdU staining was done with Imaging Kits. Apoptotic IECs were detected with *in situ* apoptotic labelling kit and results were expressed as TUNEL-positive IECs per regenerated crypts (Han et al., 2009). Images were captured using a Zeiss microscope and Axioviewer image analysis software (Carl Zeiss Corp, Germany).

Flow Cytometry (FACS). LGR5 FACS analysis was performed by using isolated ileal epithelia from *Lgr5Cre*ER and *VilCre*ER;*Lgr5Cre*ER;*Stat5*$^{f/f}$ mice. IECs were extracted with 2 mM EDTA and manual shaking, followed by cell strainer filter to generate a single-cell suspension. Singlet discrimination was sequentially performed by using plots for FSC (FSC-A vs. FSC-H) and SSC (SSC-W vs. SSC-H). Dead cells were excluded by scatter characteristics and 7-AAD staining. LGR5^{+} IESCs were identified by their endogenous GFP expression, and EdU^{+} proliferation was measured with Click-iT® FACS kit. All FACS experiments were performed on an LSR II flow Cytometer (BD Biosciences) at the CCHMC FACS Facility, and FACS data were analyzed by using FlowJo software (Tree Star, OR) (Gilbert et al., 2012; Yan et al., 2012).

Laser Capture Microdissection (LCM). Briefly, approximately 200 crypts at the very bottom of ileum from 0 position to +4 or +6 were captured by a Veritas Microdissection System (Life Technologies); RNA was isolated with a PicoPure RNA Isolation kit (Arcturus, Life Technologies) using published methods(Gilbert et al., 2012). The quality and concentration of RNA were measured by NanoDrop (Thermo Fisher, Waltham, MA). Total RNA (200 ng) was used to reversely transcribe to cDNA followed by a SYBR Green real-time PCR on the Mx4000 multiplex quantitative PCR instrument (Stratagene, La Jolla, CA).

Chromatin Immunoprecipitation (ChIP) Assay and Quantitative Real-Time PCR (qPCR). ChIP assay with sub-confluent Caco-2 cells was performed using the EZ-ChIP kit according to the manufacturer's protocol (Upstate Biotechnology). Briefly, cell lysates were extracted from sub-confluent Caco-2 cells (5×10^5 cells/ml), and anti-STAT5a or STAT5 (sc-1081 or sc-835, Santa Cruz) was used for chromatin immunoprecipitation. The chromatin precipitates were used as a template for qPCR. The STAT5 binding sites in human *BMI1* promoter and primer sequences are listed in the Supplemental Table 1.

Ileal crypts were isolated from Tam-icS5 and Tam-*RsCre*ER;icS5 mice (Spence et al., 2011). Dynabeads Protein G, mouse IgG and anti-FLAG were used to immunoprecipitate the sheered chromatin complexes. The chromatin precipitates from IgG, 1/10 input and anti-FLAG were amplified by qPCR to analyze the STAT5 binding sites in mouse *Bmi1* promoter. STAT5 binding sites and primer sequences specific for the STAT5 binding sites are listed in the Supplemental Table 2.

qPCR was performed by using the Brilliant II SYBR Green PCR Master Mix (Stratagene) as described earlier (Gilbert et al., 2012). Recovery of genomic DNA as a percentage input was calculated as the ratio of copy numbers in the precipitated immune complexes to the input control.

Total RNA was extracted from mouse tissues or cultured enteroids using RNeasy Mini Kit (QIAGEN, Valencia, CA) according to the manufacturer's protocol. PCR reactions were performed with SYBR Green QPCR mix in the Mx3000p thermocycler (Stratagene) (Gilbert et al., 2012). The primer sequences (Aguilera et al., 2011; Gilbert et al., 2012; Yui et al., 2012) are listed in the Supplemental Table 3.

Human embryonic stem cell (hESC) maintenance, Lentiviral transduction of ES cells and IEC lines.

Federally-approved WA01 (H1) hESCs were maintained in mTeSR1 media as colonies using human hESC-qualified matrigel (BD Biosciences) and passaged with 1 mg/mL dispase (Life Technologies) every 4 days. Details were described as published (McCracken et al., 2011). The plasmids **(**pMSCV-STAT5a-ER* or pMSCV-icS5-ER*) (Figure S6A) (Grebien et al., 2008) were cloned into pLENTI-PGK-Puro-DEST plasmids (Addgene, Cambridge, MA) using pENTR/D-TOPO cloning kit. STAT5a-ER* or icS5-ER* inserts were then transferred from the entry clone to the destination lentiviral plasmid pLENTI-PGK-Puro-DEST (w529-2) using lambda reverse standard recombination. The resulting lentiviral plasmids were designated: Lenti PGK Puro-STAT5a-ER* or icS5-ER*. Sub-confluent Caco-2 cells (under 25% confluency) or ES cells were respectively co-transfected with the above lentiviral plasmids combined with psPAX2 and pMD2 (Addgene, Cambridge, MA). Expression of IESC marker (LGR5) was determined with immunoblotting and PCR after STAT5 activation was induced by 4HT.

Generation of transgenic mice with inducible expression of a gain of function *Stat5* variant.

Firstly, plasmid construct targeting the icS5 (icS5-FLAG-IRES-hCD2) was generated. The 3' and 5' homologous arm (HA) with LoxP sites were amplified from BAC RP23-362J7, and icS5 gene with FLAG tag was also amplified by PCR from the pMSCV-icS5 plasmid. The 'IRES-hCD2t-SV40polyA-FRT-Kan-FRT' cassette was cloned from the pQS-CD19-hCD2t plasmid (Delogu et al., 2006). The entire construct was assembled in the pQS1 plasmid (Figure S4A). The orientation of the HA sequences was designed such that the recombined BAC contains the icS5 sequence in the anti-sense 'off' orientation. icS5-FLAG-IRES-hCD2 was then cloned into the retroviral pMSCV backbone to transfect NIH-3T3 cells or 293T cells. hCD2 expression was

detected by FACS, and the DNA binding ability of icS5 was determined by Electrophoretic Mobility Shift Assay (EMSA).

Secondly, ET recombination into BAC RP23-362J7 was performed as published (Muyrers et al., 1999). The kanamycin resistance cassette was excised by electroporation of bacterial cells containing the BAC with the 705-Flp plasmid. The final BAC harbors the icS5-FLAG-IRES-hCD2 construct, flanked by LoxP sites, in an antisense orientation within the endogenous *Stat5a* locus. The HAs allow specific recombination of the BAC, where in the start codon of the first exon of *Stat5a* was replaced by the construct. This allows expression of the icS5 construct under the regulation of the endogenous promoter upon Cre recombination (Figure 4A). The final BAC construct was confirmed by two independent Southern blots (Figure S4B). The BAC also contains the entire wild type murine *Stat5b* locus, and only 3' region of the *Stat3* locus that lacks the promoter, ATG START codon, KOZAK sequence, etc. Therefore, only STAT5 is expressed from this BAC since the 5' regulatory regions of *Stat3* locus are missing.

Thirdly, icS5 transgenic mice were generated. Briefly, the BAC construct was linearized with NotI restriction digestion and purified. 1-2 ng of the purified, linearized transgene was injected into the male pro-nuclei of fertilized eggs from C57BL/6N mice. Embryos were implanted into pseudo-pregnant females. Transgenic pups were genotyped before they were weaned (Figure S4C). Two copies of the BAC integration were confirmed by Southern blot in the transgenic mice (Figure S4D).

Finally, the mice with inducible activation of STAT5 were generated by crossing icS5 with *Rosa26-Cre*ER^{T2} mice (*RsCre*ER;icS5). Activation of STAT5 was induced by Cre-LoxP recombination, which allows the expression of icS5 upon Tam induction (Hameyer et al., 2007) (Figure 4A, and Figure S4E and 4F).

Supplemental References

Aguilera, C., Nakagawa, K., Sancho, R., Chakraborty, A., Hendrich, B., and Behrens, A. (2011). c-Jun N-terminal phosphorylation antagonises recruitment of the Mbd3/NuRD repressor complex. Nature *469*, 231-235.

Akpolat, M., Kanter, M., and Uzal, M.C. (2009). Protective effects of curcumin against gamma radiation-induced ileal mucosal damage. Archives of toxicology *83*, 609-617.

Barker, N., van Es, J.H., Kuipers, J., Kujala, P., van den Born, M., Cozijnsen, M., Haegebarth, A., Korving, J., Begthel, H., Peters, P.J., *et al.* (2007). Identification of stem cells in small intestine and colon by marker gene Lgr5. Nature *449*, 1003-1007.

Cui, Y., Riedlinger, G., Miyoshi, K., Tang, W., Li, C., Deng, C.X., Robinson, G.W., and Hennighausen, L. (2004). Inactivation of Stat5 in mouse mammary epithelium during pregnancy reveals distinct functions in cell proliferation, survival, and differentiation. Molecular and cellular biology *24*, 8037-8047.

Delogu, A., Schebesta, A., Sun, Q., Aschenbrenner, K., Perlot, T., and Busslinger, M. (2006). Gene repression by Pax5 in B cells is essential for blood cell homeostasis and is reversed in plasma cells. Immunity *24*, 269-281.

el Marjou, F., Janssen, K.P., Chang, B.H., Li, M., Hindie, V., Chan, L., Louvard, D., Chambon, P., Metzger, D., and Robine, S. (2004). Tissue-specific and inducible Cre-mediated recombination in the gut epithelium. Genesis *39*, 186-193.

Gilbert, S., Zhang, R., Denson, L., Moriggl, R., Steinbrecher, K., Shroyer, N., Lin, J., and Han, X. (2012). Enterocyte STAT5 promotes mucosal wound healing via suppression of myosin light chain kinase-mediated loss of barrier function and inflammation. EMBO Mol Med,2012;4(2):109-24.

Grebien, F., Kerenyi, M.A., Kovacic, B., Kolbe, T., Becker, V., Dolznig, H., Pfeffer, K., Klingmuller, U., Muller, M., Beug, H., *et al.* (2008). Stat5 activation enables erythropoiesis in the absence of EpoR and Jak2. Blood *111*, 4511-4522.

Gregorieff, A., and Clevers, H. (2010). In situ hybridization to identify gut stem cells. Current protocols in stem cell biology *Chapter 2*, Unit 2F 1.

Hameyer, D., Loonstra, A., Eshkind, L., Schmitt, S., Antunes, C., Groen, A., Bindels, E., Jonkers, J., Krimpenfort, P., Meuwissen, R., *et al.* (2007). Toxicity of ligand-dependent Cre recombinases and generation of a conditional Cre deleter mouse allowing mosaic recombination in peripheral tissues. Physiological genomics *31*, 32-41.

Han, X., Gilbert, S., Groschwitz, K., Hogan, S., Jurickova, I., Trapnell, B., Samson, C., and Gully, J. (2010). Loss of GM-CSF signalling in non-haematopoietic cells increases NSAID ileal injury. Gut *59*, 1066-1078.

Han, X., Ren, X., Jurickova, I., Groschwitz, K., Pasternak, B.A., Xu, H., Wilson, T.A., Hogan, S.P., and Denson, L.A. (2009). Regulation of intestinal barrier function by signal transducer and activator of transcription 5b. Gut *58*, 49-58.

Hua, G., Thin, T.H., Feldman, R., Haimovitz-Friedman, A., Clevers, H., Fuks, Z., and Kolesnick, R. (2012). Crypt base columnar stem cells in small intestines of mice are radioresistant. Gastroenterology *143*, 1266-1276.

Kim, T.H., Escudero, S., and Shivdasani, R.A. (2012). Intact function of Lgr5 receptor-expressing intestinal stem cells in the absence of Paneth cells. Proceedings of the National Academy of Sciences of the United States of America *109*, 3932-3937.

McCracken, K.W., Howell, J.C., Wells, J.M., and Spence, J.R. (2011). Generating human intestinal tissue from pluripotent stem cells in vitro. Nat Protoc *6*, 1920-1928.

Melendez, J., Liu, M., Sampson, L., Akunuru, S., Han, X., Vallance, J., Witte, D., Shroyer, N., and Zheng, Y. (2013). Cdc42 coordinates proliferation, polarity, migration, and differentiation of small intestinal epithelial cells in mice. Gastroenterology *145*, 808-819.

Munoz, J., Stange, D.E., Schepers, A.G., van de Wetering, M., Koo, B.K., Itzkovitz, S., Volckmann, R., Kung, K.S., Koster, J., Radulescu, S., *et al.* (2012). The Lgr5 intestinal stem cell signature: robust expression of proposed quiescent '+4' cell markers. The EMBO journal *31*, 3079-3091.

Muyrers, J.P., Zhang, Y., Testa, G., and Stewart, A.F. (1999). Rapid modification of bacterial artificial chromosomes by ET-recombination. Nucleic acids research *27*, 1555-1557.
Sato, T., Vries, R.G., Snippert, H.J., van de Wetering, M., Barker, N., Stange, D.E., van Es, J.H., Abo, A., Kujala, P., Peters, P.J., *et al.* (2009). Single Lgr5 stem cells build crypt-villus structures in vitro without a mesenchymal niche. Nature *459*, 262-265.
Spence, J.R., Mayhew, C.N., Rankin, S.A., Kuhar, M.F., Vallance, J.E., Tolle, K., Hoskins, E.E., Kalinichenko, V.V., Wells, S.I., Zorn, A.M., *et al.* (2011). Directed differentiation of human pluripotent stem cells into intestinal tissue in vitro. Nature,2011;470(7332):105-9.
Wong, V.W., Stange, D.E., Page, M.E., Buczacki, S., Wabik, A., Itami, S., van de Wetering, M., Poulsom, R., Wright, N.A., Trotter, M.W., *et al.* (2012). Lrig1 controls intestinal stem-cell homeostasis by negative regulation of ErbB signalling. Nature cell biology *14*, 401-408.
Yan, K.S., Chia, L.A., Li, X., Ootani, A., Su, J., Lee, J.Y., Su, N., Luo, Y., Heilshorn, S.C., Amieva, M.R., *et al.* (2012). The intestinal stem cell markers Bmi1 and Lgr5 identify two functionally distinct populations. Proceedings of the National Academy of Sciences of the United States of America *109*, 466-471.
Yui, S., Nakamura, T., Sato, T., Nemoto, Y., Mizutani, T., Zheng, X., Ichinose, S., Nagaishi, T., Okamoto, R., Tsuchiya, K., *et al.* (2012). Functional engraftment of colon epithelium expanded in vitro from a single adult Lgr5(+) stem cell. Nature medicine,2011 Sep;32(26):6342-50.